Bounds to the pull-in voltage of a MEMS/NEMS beam with surface elasticity

Please use this PDF proof to check the layout of your article. If you would like any changes to be made to the layout, you can leave instructions in the online proofing interface. First, return to the online proofing interface by clicking "Edit" at the top page, then insert a Comment in the relevant location. Making your changes directly in the online proofing interface is the quickest, easiest way to correct and submit your proof.

Please note that changes made to the article in the online proofing interface will be added to the article before publication, but are not reflected in this PDF proof.

Applied Mathematical Modelling xxx (xxxx) xxx

Contents lists available at ScienceDirect

Applied Mathematical Modelling

journal homepage: www.elsevier.com/locate/apm

Bounds to the pull-in voltage of a MEMS/NEMS beam with surface elasticity

Q1 Enrico Radi[a,b], Giovanni Bianchi[a,b], Andrea Nobili[b,c,*]

[a] Dipartimento di Scienze e Metodi dell'Ingegneria, Università di Modena e Reggio Emilia, Via Amendola, 2, 42122 Reggio Emilia, Italy
[b] Centro Interdipartimentale "En&Tech", via G. Amendola, 2, Reggio Emilia 42122, Italy
Q2 [c] Dipartimento di Ingegneria "Enzo Ferrari", Università di Modena e Reggio Emilia, Via Vivarelli, 10, 41125 Modena, Italy

ARTICLE INFO

Article history:
Received 21 April 2020
Revised 9 October 2020
Accepted 17 October 2020
Available online xxx

Keywords:
Pull-in instability
Electro-mechanical nano-switch
Surface elasticity
NEMS

ABSTRACT

The problem of pull-in instability of a cantilever micro- or nano-switch under electrostatic forces has attracted considerable attention in the literature, given its importance in designing micro- and nano-electromechanical systems (MEMS and NEMS). The non-linear nature of the problem supports the typical approach that relies on numerical or semi-analytical tools to approximate the solution.

By contrast, we determine fully analytical upper and lower bounds to the pull-in instability phenomenon for a cantilever beam under the action of electrostatic, van der Waals or Casimir forces. In particular, the novel contribution of this works consists in accounting for size effects analytically, in the spirit of surface elasticity, which adds considerable complication to the problem, allowing for a nonconvex beam deflection. Surface energy effects are generally ignored in classical elasticity, although they are known to become relevant for very small structures and especially at the nano-scale, owing to their large surface/volume ratio. Closed form lower and upper bounds are given for the pull-in characteristics, that allow to discuss the role of several tuneable parameters. Indeed, the evolution of the cantilever tip deflection is presented as a function of the applied voltage up to the occurrence of pull-in and the contribution of van der Waals and Casimir intermolecular interactions is discussed. It is found that intermolecular forces strongly decrease the pull-in voltage, while surface elasticity works in the opposite direction and stabilizes the system. The accuracy of the bounding solutions, measured in terms of the difference between upper and lower analytical bounds, is generally very good, although it rapidly deteriorates as the effect of surface elasticity becomes more pronounced. Finally, approximated closed-form relations are developed to yield simple and accurate design formulae: in particular, they provide estimates for the minimum theoretical gap and for the maximum operable length for a free-standing cantilever in the presence of the effects of surface elasticity and intermolecular interactions. Results may be especially useful for designing and optimizing NEMS switches.

1. Introduction

Electrostatic bistable switches are widely available components of micro- and nanoelectromechanical systems (respectively MEMS and NEMS), as they serve under multiple purposes: for instance they may act as sensing, actuating, information

Q3 * Corresponding author at: Centro Interdipartimentale "En&Tech", via G. Amendola, 2, Reggio Emilia 42122, Italy.
E-mail address: andrea.nobili@unimore.it (A. Nobili).

https://doi.org/10.1016/j.apm.2020.10.031
0307-904X/

Q4 storing, signal filtering or resonating devices ([1], Ionescu, 2014). In the form of actuators, they generally appear as pairs of electrodes, one fixed and embedded in a support, the other movable and in the shape of a beam, that are operated by the application of a driving electrostatic potential. In dependence of this, the movable electrode deflects until a threshold voltage is reached, namely the pull-in voltage, which causes the beam to suddenly collapse onto the ground electrode. It is precisely the design of the pull-in voltage (and, consequently, of the pull-in gap, that is the minimum gap sitting between the electrodes right before pull-in kicks in) that is the fundamental feature of the actuator.

Indeed, a large pull-in voltage allows for great deflection and therefore control, and yet it drains large amounts of energy. Conversely, designing for small pull-in voltages affords efficient and fast operation, although the device becomes now susceptible to manufacturing defects, which may easily trigger the switch unexpectedly. This is especially true for NEMS, for which intermolecular action, such as van der Waals (vdW) or Casimir forces, takes on a relevant part in the mechanics of actuation. In fact, at the distance of tens of nanometers, typical of NEMS, very short range forces become comparable in magnitude to the electrostatic force.

Also, the effect of surface free energy becomes especially important in the case of nano-scale elements. Indeed, the large surface-to-volume ratio of these requires that surface energy effects be taken into consideration, the energy associated with atoms at or near a free surface being different from that of atoms in the bulk. Consequently, the study of the elastic behavior of a nanobeam with surface energy effects is relevant for many current technological developments.

Furthermore, at the micro- and, even more, at the nano-scale, size effects deeply affect mechanical performance of the flexible electrode and classical elastic theory produce unreliable results [2,3]. Experiments performed by Sadeghian et al. [4] show that pull-in instability of nanobeams is indeed size-dependent. Therefore, an improved beam model incorporating the contribution of the size effect is required for accurate modelling of MEMS and, especially, NEMS.

Several strategies are available to incorporate size effects: through polar theories, such as couple-stress or modified couple stress [5], through introducing surface elastic energy [6–12, 3] or by means of non-local theories [13–16]. Surface elastic energy was introduced by Gurtin and Murdoch [17,18] to account for the apparent increase of the elastic modulus when scaling down samples, owing to surface tension. This effect is measured by Cuenot et al. [7] by Atomic Force Microscopy (AFM) and by McFarland et al. [11] for the natural frequency of micro-cantilever beams. He and Lilley, [9] incorporate this contribution within the classical theory of bending and compare the outcomes of this new model with static bending tests for nano-wires. Similarly, Wang and Feng [3] investigate the contribution of surface elastic energy to buckling of nanobeams, Park [12] considers buckling strains of silicon nano-wires and Challamel and Elishakoff [6] extend the instability analysis to Timoshenko beam theories.

An alternative approach for studying the mechanics of nano-scale structures and devices is based on atomistic modelling. This, however, requires a very substantial computational effort and thus adoption of continuum-based models allows for simple and efficient designing tools.

The development of analytical models able to predict the pull-in voltage of micro- and nano-devices is extremely important for assuring efficient and consistent performance, while preventing unexpected structural failure [19].

Unfortunately, the inherently nonlinear nature of the operating forces prevents from developing a closed-form solution to put to advantage at the design and at the optimization stage.

Instead, a large amount of numerical or semi-numerical approaches are presented in the literature.

Zhang and Zhao [20] present a one-degree-of-freedom (lumped) system analysis that is extended to a cantilever beam with mid-plane stretching by Taylor expanding the electrostatic action; the resulting integro-differential equation is solved, with a one-mode approximation, by taking the transversal displacement proportional to the first vibration mode for a cantilever. In similar fashion, Ramezani et al. [21,22] provide an estimation of the pull-in voltage by adopting the Green's function of the linear differential operator and then resorting to a quadratic shape for the displacement. A similar analysis is presented in Baghani [5], where Casimir effects are also introduced, and in Duan and Rach [8] and Duan et al. [23], where the contribution of surface elastic energy is addressed. A semi-numerical approach is considered in Duan et al. [24], by means of a modified Adomian decomposition, that falls upon a large body of literature employing homotopy perturbation theory, see Ma et al. [10] and references therein. Fu and Zhang [25] and Wang and Wang [26,27] numerically investigate pull-in instability of a nano-cantilever switch in the presence of surface elastic energy also accounting for geometric nonlinearity for the beam curvature.

All contributions available in the literature eventually resort to numerical methods for approximating the solution. In contrast, Radi et al. [28,29] introduce a purely analytical technique that relies on careful estimates of the beam deflection and provides sharp lower and upper bounds along the cantilever deflection until pull-in kicks in. Closed form solutions are especially valuable for they retain full information on the role of the problem's parameters. This method is successfully applied to a MEM/NEM cantilever under electrostatic, vdW and Casimir forces, considering the effect of an elastic constraint [28], and a compressive axial load [29]. Recently, this approach has been extended to investigate the pull-in instability of carbon nanotubes under electrostatic actuation [30]. It is important to emphasize that a common feature of these works is that size effects are neglected, so that the deflection of the system is always convex and much of the analysis relies thereon.

As a novel contribution with respect to the previous papers, here we stretch the method to account for surface elastic energy, which substantially affects the beam stiffness at very small scales. In contrast to a compressive axial force, the contribution of surface elastic energy is associated with the second derivative of the transversal displacement via a negative sign. This feature is a substantial obstacle to the application of the method, we can indeed no longer prove that the deflection is convex (Section 2). Still, enough insight into the solution is provided to build lower and upper bounds to the

beam deflection (Section 3), which are then used for bounding the pull-in parameters in Section 4. Results are discussed in Section 5, where simple closed-form relations are proposed for approximate design of the pull-in parameters, namely the minimum admissible gap and the maximum operable length for a free-standing cantilever, in the presence of the effects of surface elasticity and intermolecular interactions. Finally, conclusions are drawn in Section 6.

2. Mathematical model

The problem of an elastic micro- or nano-cantilever, subject to electrostatic actuation encompassing the effect of the fringing field, vdW or Casimir forces and of surface elastic energy is described by the following fourth-order, non-linear ODE [31,32,10]

$$u^{\mathrm{IV}}(x) - \eta^2 u''(x) = f(u(x)), \quad \text{for } x \in [0,1], \tag{1}$$

where $u = v/d$ and $x = z/l$ are nondimensional variables, v is the beam deflection, d the initial gap between the electrodes, l the beam length, $0 \le z \le l$ the position along the beam as measured from the clamped end, and prime denotes differentiation with respect to the function argument. The non-dimensional positive parameter

$$\eta^2 = \frac{2\, w\, \tau_0\, L^2}{EI_{eff}}, \tag{2}$$

takes into account the surface energy effect [31], where τ_0 is the surface residual stress, $EI_{eff} = EI + E_s w h^2/2$ is the bending rigidity of the beam incorporating the surface elasticity effect, being w and h the width and height of the nanobeam cross section, E the Young's modulus of the elastic material, I the moment of inertia of the beam cross-section, and E_s the surface elastic modulus.

The loading term in (1) includes the contributions of electrostatic actuation, fringing field, vdW and Casimir forces, respectively

$$f(u) = \frac{\gamma\, \beta}{1-u} + \frac{\beta}{(1-u)^2} + \frac{\alpha_W}{(1-u)^3} + \frac{\alpha_C}{(1-u)^4}, \tag{3}$$

being $\gamma = 0.65 d/w$ the fringing coefficient. The nondimensional parameters β, α_W, and α_C are given by

$$\beta = \frac{\varepsilon_0\, w V^2 l^4}{2\, d^3 EI_{eff}}, \quad \alpha_W = \frac{A\, w\, l^4}{6\pi\, d^4 EI_{eff}}, \quad \alpha_C = \frac{\pi^2 h\, c\, w\, l^4}{240\, d^5 EI_{eff}}, \tag{4}$$

where V is the electric voltage applied to the electrodes, $\varepsilon_0 = 8.854 \cdot 10^{-12} C^2 N^{-1} m^{-2}$ is the permittivity of vacuum, A is the Hamaker constant, $h = 1.055 \cdot 10^{-34} Js$ is the Planck's constant divided by 2π, $c = 2.998 \cdot 10^8$ m/s is the speed of light.

Let us denote with $\delta = u(1)$ the cantilever tip deflection, then the following inequalities hold for the functions $f(u)$ and $f'(u)$

$$0 \le f(0) \le f(u) \le f(\delta), \quad 0 \le f'(0) \le f'(u) \le f'(\delta), \quad \text{for } 0 \le u \le \delta, \tag{5}$$

where

$$f'(u) = \frac{\gamma\, \beta}{(1-u)^2} + \frac{2\beta}{(1-u)^3} + \frac{3\alpha_W}{(1-u)^4} + \frac{4\alpha_C}{(1-u)^5}, \tag{6}$$

The boundary conditions for a cantilever beam require that displacement and rotation vanish at the built-in cross section $x = 0$, while bending moment and shearing force disappear at the free end $x = 1$, namely [31]

$$u(0) = 0, \quad u'(0) = 0, \quad u''(1) = 0, \quad u'''(1) - \eta^2 u'(1) = 0, \tag{7}$$

Note that Koochi et al. [32] in their investigation considered the boundary condition $u'''(1) = 0$ instead of $(7)_4$. Integrating the governing ODE (1) between x and 1 and using the boundary condition $(7)_4$ yields

$$-u'''(x) + \eta^2 u'(x) = \int_x^1 f(u(t))\, dt \ge (1-x) f(0). \tag{8}$$

the inequality having being obtained making use of $(5)_1$. Likewise, integrating again, taking advantage of the boundary condition $(7)_3$ and exploiting integration by parts yields

$$u''(x) + \eta^2 [\delta - u(x)] = \int_x^1 (t-x) f(u(t))\, dt \ge \frac{1}{2}(1-x)^2 f(0). \tag{9}$$

2.1. Nonlinear integral equation formulation

We begin by seeking bounds for the beam transversal displacement and its derivatives. To this aim, we adopt an integral representation for the displacement through the problem's Green function. The Green function for a cantilever beam with surface energy is obtained solving the following linear ODE

$$G^{\mathrm{IV}}(t) - \eta^2 G''(t) = \delta(x-t) \tag{10}$$

The general solution to the ODE (10) is

$$G(t) = \begin{cases} A_0 + A_1 t + A_2 \cosh \eta t + A_3 \sinh \eta t, & 0 \le t < x, \\ B_0 + B_1 t + B_2 \cosh \eta t + B_3 \sinh \eta t, & x < t \le 1. \end{cases} \tag{11}$$

where the eight coefficients A_i and B_i ($i=0, 1, 2, 3$) are determined by imposing the boundary conditions (7) at the ends $t=0,1$, together with continuity across $t=x$ for the function and its derivatives up to the second order. Furthermore, we impose the jump condition

$$G'''\left(x^+\right) - \eta^2 G'\left(x^+\right) - G'''\left(x^-\right) + \eta^2 G'\left(x^-\right) = 1, \tag{12}$$

thus yielding

$$G(t) = \begin{cases} \{\eta t - \sinh \eta t + (\cosh \eta t - 1)[\sinh \eta x - (\cosh \eta x - 1)\tanh \eta]\}/\eta^3, & 0 \le t < x, \\ \{\eta x - \sinh \eta x + (\cosh \eta x - 1)[\sinh \eta t - (\cosh \eta t - 1)\tanh \eta]\}/\eta^3, & x < t \le 1. \end{cases} \tag{13}$$

Therefore, by using the Green's function (13), the BVP defined by (1) and (7) can be equivalently formulated in term of the following non-linear integral equation

$$\begin{aligned} u(x) = {} & \tfrac{1}{\eta^3} \int_0^x \{\eta t - \sinh \eta t + (\cosh \eta t - 1)[\sinh \eta x - (\cosh \eta x - 1)\tanh \eta]\} f(u(t)) dt \\ & + \tfrac{1}{\eta^3} \int_x^1 \{\eta x - \sinh \eta x + (\cosh \eta x - 1)[\sinh \eta t - (\cosh \eta t - 1)\tanh \eta]\} f(u(t)) dt. \end{aligned} \tag{14}$$

An integral expression for the normalized cantilever tip deflection $\delta = u(1)$ naturally follows from (14)

$$\delta = \frac{1}{\eta^3} \int_0^1 [\eta t - \sinh \eta t + (\cosh \eta t - 1)\tanh \eta] f(u(t)) dt. \tag{15}$$

Recalling that $\tanh \eta < 1$, we can write the estimates

$$\begin{aligned} & \eta t - \sinh \eta t + (\cosh \eta t - 1)[\sinh \eta x - (\cosh \eta x - 1)\tanh \eta] \ge \\ & \quad \ge \eta t - \sinh \eta t + (\cosh \eta t - 1)(\sinh \eta x - \cosh \eta x + 1) \\ & \quad \ge \eta t - \sinh \eta t + (\cosh \eta t - 1)(\sinh \eta t - \cosh \eta t + 1) \ge 0, \end{aligned} \tag{16}$$

for $0 \le t \le x \le 1$, and

$$\begin{aligned} & \eta x - \sinh \eta x + (\cosh \eta x - 1)[\sinh \eta t - (\cosh \eta t - 1)\tanh \eta] \ge \\ & \quad \ge \eta x - \sinh \eta x + (\cosh \eta x - 1)(\sinh \eta t - \cosh \eta t + 1) \\ & \quad \ge \eta x - \sinh \eta x + (\cosh \eta x - 1)(\sinh \eta x - \cosh \eta x + 1) \ge 0, \end{aligned} \tag{17}$$

for $0 \le x \le t \le 1$. These inequalities, plugged into (14), immediately prove that the function $u(x)$ is positive. Indeed, in light of $(5)_1$, we obtain the lower bound

$$u(x) \ge A(x) f(0) \ge 0, \tag{18}$$

having let the positive function

$$\begin{aligned} A(x) = {} & \frac{1}{\eta^3} \int_0^x \{\eta t - \sinh \eta t + (\cosh \eta t - 1)[\sinh \eta x - (\cosh \eta x - 1)\tanh \eta]\} dt \\ & + \frac{1}{\eta^3} \int_x^1 \{\eta x - \sinh \eta x + (\cosh \eta x - 1)[\sinh \eta t - (\cosh \eta t - 1)\tanh \eta]\} dt \\ = {} & \frac{1}{\eta^2} \left[x - \frac{x^2}{2} + \frac{\cosh \eta x - 1 - \eta \sin \eta + \eta \sinh \eta (1 - x)}{\eta^2 \cosh \eta} \right]. \end{aligned} \tag{19}$$

Looking at the derivative of Eq. (14), one obtains

$$\begin{aligned} u'(x) = {} & \frac{\cosh \eta x - \sinh \eta x \tanh \eta}{\eta^2} \int_0^x (\cosh \eta t - 1) f(u(t)) dt \\ & + \frac{1}{\eta^2} \int_x^1 \{[\sinh \eta t - (\cosh \eta t - 1)\tanh \eta] \sinh \eta x - \cosh \eta x + 1\} f(u(t)) dt, \end{aligned} \tag{20}$$

and the function under the first integral is non-negative, given that $\cosh \eta t \ge 1$. For the function in the second integral, we have the estimate

$$\begin{aligned} & [\sinh \eta t - (\cosh \eta t - 1)\tanh \eta] \sinh \eta x - \cosh \eta x + 1 \ge (\sinh \eta t - \cosh \eta t + 1) \sinh \eta x - \cosh \eta x + 1 \ge \\ & \quad \ge (\sinh \eta x - \cosh \eta x + 1) \sinh \eta x - \cosh \eta x + 1 = \sinh^2 \eta x - (\cosh \eta x - 1)(\sinh \eta x + 1) \ge \\ & \quad \ge \sinh^2 \eta x - \cosh^2 \eta x + 1 = 0 \end{aligned} \tag{21}$$

whereby $u'(x) \ge 0$ and $u(x)$ is monotonic increasing. As a consequence, $0 \le u(x) \le \delta$ and $0 \le f(0) \le f(u) \le f(\delta)$. Immediately, we have the bound

$$u'(x) \ge B(x) f(0) \ge 0, \tag{22}$$

where we let the positive function

$$B(x) = A'(x) = \frac{1}{\eta^2}\left[1 - x - \frac{\cosh\eta(1-x)}{\cosh\eta} + \frac{\sinh\eta x}{\eta\cosh\eta}\right]. \tag{23}$$

Furthermore, from Eq. (20) evaluated at $x=1$ and from condition $(5)_1$, one readily has the upper bound

$$u'(1) \le \frac{1}{\eta^2\cosh\eta}\int_0^1 (\cosh\eta t - 1)dt\, f(\delta) = \frac{\sinh\eta - \eta}{\eta^3\cosh\eta} f(\delta). \tag{24}$$

Turning now to the second derivative

$$u''(x) = \frac{\sinh\eta x - \cosh\eta x\tanh\eta}{\eta}\int_0^x (\cosh\eta t - 1) f(u(t))dt + \frac{1}{\eta}\int_x^1 \{[\sinh\eta t - (\cosh\eta t - 1)\tanh\eta]\ \cosh\eta x - \sinh\eta x\} f(u(t))dt, \tag{25}$$

we have that

$$\sinh\eta x - \cosh\eta x\tanh\eta = (\tanh\eta x - \tanh\eta)\cosh\eta x \le 0, \quad \text{for } x \le 1, \tag{26}$$

whence nothing can be said in general on the sign of $u''(x)$. Indeed, surface energy opposes a simple convex deformation for the cantilever and this makes the analysis considerably harder.

In fact, the function u is positive and increasing, namely $u(x) \ge 0$ and $u'(x) \ge 0$, but not necessarily convex, being $u''(x)$ not defined in sign.

For the third derivative

$$u'''(x) = (\cosh\eta x - \sinh\eta x\tanh\eta)\int_0^x (\cosh\eta t - 1) f(u(t))dt + \int_x^1 \{[\sinh\eta t - (\cosh\eta t - 1)\tanh\eta]\ \sinh\eta x - \cosh\eta x\} f(u(t))dt. \tag{27}$$

we observe that

$$[\sinh\eta t - (\cosh\eta t - 1)\tanh\eta]\ \sinh\eta x - \cosh\eta x \le [\sinh\eta t - (\cosh\eta t - 1)\tanh\eta t]\ \sinh\eta x - \cosh\eta x = (\tanh\eta t\ \tanh\eta x - 1)\cosh\eta x \le 0, \tag{28}$$

for $0 \le x \le t \le 1$, and

$$\cosh\eta x - \sinh\eta x\tanh\eta = (1 - \tanh\eta x\tanh\eta)\ \cosh\eta x \ge 0, \tag{29}$$

for $0 \le x \le 1$, whence, again, nothing can be said in general on the sign of $u'''(x)$, since the first term of (27) is positive and the second is negative. Still, we can write the lower bound

$$u'''(x) \ge C(x)f(0) - D(x)f(\delta), \quad \text{for } 0 < x < 1. \tag{30}$$

where we have let

$$C(x) = (\cosh\eta x - \sinh\eta x\tanh\eta)\int_0^x (\cosh\eta t - 1)dt = \frac{1}{\eta}(\cosh\eta x - \sinh\eta x\tanh\eta)(\sinh\eta x - \eta x),$$
$$D(x) = -\int_x^1 \{[\sinh\eta t - (\cosh\eta t - 1)\tanh\eta]\ \sinh\eta x - \cosh\eta x\}dt = = \frac{(\eta - \eta x + \sinh\eta x)\ \cosh\eta(1-x) - \sinh\eta x}{\eta\ \cosh\eta}, \tag{31}$$

Indeed, the functions $C(x)$ and $D(x) \ge 0$ are positive, for $0 \le x \le 1$ and $\eta \ge 0$, and use have been made of inequality $(5)_1$.

3. A priori estimates on the beam deflection

In order to define upper and lower bounds on the pull-in parameters, two-sided estimates are derived for the deflection $u(x)$, that is the solution to the BVP defined by conditions (1) and (7).

To this aim, we employ lemmas A and B given in the Appendix, which were already introduced in [28,29]. Lemma A provides the upper bound for $u(x)$ and requires defining a function $h(x)$ such that $h^{\mathrm{V}}(x) \le 0$. For this, we observe that, from Eq. (1) and making use of the estimates (22) and (30),

$$u^{\mathrm{V}}(x) = u'(x)f'(u) + \eta^2 u'''(x) \ge B(x)f(0)f'(0) + \eta^2[C(x)f(0) - D(x)f(\delta)], \tag{32}$$

whereupon it easily follows

$$h^{\mathrm{V}}(x) = B(x)f(0)f'(0) + \eta^2\left[C(x)f(0) - D(x)f(\delta) - u^{\mathrm{V}}(x) \le 0\right]. \tag{33}$$

Let us now define the functions $a(x)$, $b(x)$, $c(x)$ and $d(x)$ such that

$$a^{\mathrm{IV}}(x) = A(x), \quad b^{\mathrm{V}}(x) = B(x), \quad c^{\mathrm{V}}(x) = C(x), \quad d^{\mathrm{V}}(x) = D(x), \tag{34}$$

Clearly, $a(x)$ and $b(x)$ are the same up to a constant. The expressions for $a(x)$, $b(x)$, $c(x)$ and $d(x)$ are given in Appendix B. Integrating five times Eq. (33) by using Eq. (34), we get the function $h(x)$

$$h(x) = H(x) - u(x) + p_4(x) \tag{35}$$

where $p_4(x)$ is an arbitrary fourth-degree polynomial and we have let the shorthand

$$H(x) = b(x)f(0)f'(0) + \eta^2[c(x)f(0) - d(x)f(\delta)]. \tag{36}$$

Similarly, Lemma B provides the lower bound for $u(x)$ and demands letting a functiong(x) such that $g^{\mathrm{IV}}(x) \geq 0$. For this, we make once more use of Eq. (1) and take advantage of the estimates $(5)_1$, (9) and (18)

$$u^{\mathrm{IV}}(x) \geq \frac{\eta^2}{2}(1-x)^2 f(0) - \eta^4[\delta - u(x)] + f(0) \geq \eta^4 A(x)f(0) - \eta^4\delta + \frac{\eta^2}{2}(1-x)^2 f(0) - f(0). \tag{37}$$

Therefore, we let

$$g^{\mathrm{IV}}(x) = u^{\mathrm{IV}}(x) - \eta^4 A(x)f(0) + \eta^4\delta - \frac{\eta^2}{2}(1-x)^2 f(0) - f(0) \geq 0, \tag{38}$$

which, integrated four times, gives

$$g(x) = u(x) - \eta^4 a(x)f(0) + \frac{x^4}{24}\left[\eta^4\delta - f(0)\right] - \eta^2\frac{x^4}{720}\left(15 - 6x + x^2\right)f(0) + p_3(x) \tag{39}$$

where $p_3(x)$ is a yet unknown arbitrary polynomial of third degree.

3.1. Upper bound for the deflection u(x)

The explicit form for the yet undetermined polynomial $p_4(x)$ is determined so as to satisfy the boundary conditions for $h(x)$ given in Lemma A, namely

$$h(0) = 0, \quad h(1) = 0, \quad h'(0) = 0, \quad h''(1) = 0, \quad h'''(1) = 0, \tag{40}$$

By using the BCs (7), the function $h(x)$ defined in (35) that satisfies conditions (33) and (40) then writes

$$\begin{aligned} h(x) = {} & H(x) - H(0) - xH'(0) - \frac{1}{2}H''(1) + \frac{1}{3}\left(6x^2 - 4x^3 + x^4\right)\left[\delta + H(0) - H(1) + H'(0) + \frac{1}{2}H''(1)\right] \\ & + \frac{1}{18}\left(3x^2 - 5x^3 + 2x^4\right)\left[\eta^2 u'(1) - H'''(1)\right] - u(x) \geq 0, \end{aligned} \tag{41}$$

where the function $H(x)$ has been defined in (36). Then, by Lemma A, it is $h(x) \geq 0$ for $0 \leq x \leq 1$.

By introducing the inequality (24) for $u'(1)$ in (41) one obtains the upper bound $U(x)$ on the beam deflection $u(x)$, such that $u(x) \leq U(x)$ for $0 \leq x \leq 1$, where

$$\begin{aligned} U(x) = {} & H(x) + \frac{1}{3}\left(6x^2 - 4x^3 + x^4\right)\left[\delta + H(0) - H(1) + H'(0) + \frac{1}{2}H''(1)\right] \\ & + \frac{1}{18}\left(3x^2 - 5x^3 + 2x^4\right)\left[\frac{\sinh\eta - \eta}{\eta\cosh\eta}f(\delta) - H'''(1)\right] - H(0) - xH'(0) - \frac{1}{2}x^2 H''(1). \end{aligned} \tag{42}$$

For small values of η, one finds

$$\begin{aligned} U(x) = {} & \frac{1}{3}\left\{\left(6x^2 - 4x^3 + x^4\right)\delta - \frac{1-x}{40320}\left(294x^2 - 350x^3 + 63x^4 + 63x^5 - 21x^6 + 3x^7\right)f(0)f'(0)\right. \\ & + \frac{1-x}{720}\eta^2\left[\left(75x^2 - 65x^3 + 15x^4 - 3x^5\right)f(\delta)\right. \\ & \left.\left. + \frac{f(0)\,f'(0)}{1680}\left(3483x^2 - 3969x^3 + 594x^4 + 594x^5 - 36x^6 - 36x^7 + 9x^8 - x^9\right)\right]\right\} + O\left(\eta^2\right). \end{aligned} \tag{43}$$

3.2. Lower bounds for the deflection u(x)

The four arbitrary constants in $p_3(x)$ are chosen such that the four conditions required by lemma B

$$g(0) = 0, \quad g(1) = 0, \quad g'(0) = 0, \quad g''(1) = 0. \tag{44}$$

By using the BCs (7), the function $g(x)$ satisfying conditions (38) and (44) then writes

$$g(x) = u(x) - \frac{1}{48}\left(72 - 3\eta^4 - 24x + 5\eta^2 x - 2\eta^4 x^2\right)x^2\delta$$
$$- \frac{f(0)}{96\,\eta^4}\left[96\eta^2 x - 3\left(48 + 40\eta^2 - 2\eta^4 - \eta^6\right)x^2 + \left(48 + 24\eta^2 - 10\eta^4 + 5\eta^6\right)x^3 + 2\eta^4\left(2 + \eta^2\right)x^4\right.$$
$$\left. -2\left(48 - 72x^2 + 3\eta^4 x^2 + 24x^3 - 5\eta^4 x^3 + 2\eta^4 x^4 - 48\cosh\eta x\right)\frac{1 + \eta\sinh\eta}{\cosh\eta} - 96\eta\sinh\eta x\right] \geq 0. \quad (45)$$

Then, lemma B assures that the function $g(x)$ is non-negative in the range $0 \leq x \leq 1$. Therefore, the lower bound $L(x)$ on the beam deflection $u(x)$, such that $u(x) \geq L(x)$ for $0 \leq x \leq 1$, is given by

$$L(x) = \frac{1}{48}\left(72 - 3\eta^4 - 24x + 5\eta^2 x - 2\eta^4 x^2\right)x^2\delta$$
$$+ \frac{f(0)}{96\,\eta^4}\left[96\eta^2 x - 3\left(48 + 40\eta^2 - 2\eta^4 - \eta^6\right)x^2 + \left(48 + 24\eta^2 - 10\eta^4 + 5\eta^6\right)x^3 + 2\eta^4\left(2 + \eta^2\right)\right.$$
$$\left. -2\left(48 - 72x^2 + 3\eta^4 x^2 + 24x^3 - 5\eta^4 x^3 + 2\eta^4 x^4 - 48\cosh\eta x\right)\frac{1 + \eta\sinh\eta}{\cosh\eta} - 96\eta\sinh\eta x\right]. \quad (46)$$

For small values of η, one finds

$$L(x) = \frac{1}{2}(3 - x)x^2\delta + \frac{f(0)}{48}(1 - x)x^2\left[3 - 2x + \frac{\eta^2}{30}\left(15 - 20x + 10x^2 - 2x^3\right)\right] + O\left(\eta^4\right). \quad (47)$$

4. Lower and upper bounds on the pull-in parameters

Plugging the upper (lower) bound in expression (15) for the normalized cantilever tip deflection δ, the following upper (lower) bound can be derived for the pull-in parameters β_{PI} and δ_{PI}.

4.1. Lower bounds for the pull-in parameters

By using (42), Eq. (15) lends

$$\delta \leq \frac{1}{\eta^3}\int_0^1 \left[\eta t - \sinh\eta t + (\cosh\eta t - 1)\tanh\eta\right] f(U(t))dt, \quad (50)$$

being $f(u(t)) \leq f(U(t))$ and

$$\eta t - \sinh\eta t + (\cosh\eta t - 1)\tanh\eta > \eta t - \sinh\eta t + (\cosh\eta t - 1)\tanh\eta t = \eta t - \tanh\eta t > 0, \quad (51)$$

for $0 < t < 1$.

Inequality (50) defines a lower bound for the relation between the electrostatic loading parameter β and the normalized pull-in deflection δ, both included in $U(t)$. In particular, the maximum electrostatic load β and the corresponding tip deflection δ are to be found among stationarity points

$$\frac{\partial\beta}{\partial\delta} = 0. \quad (52)$$

This defines lower bounds for the pull-in parameters β_L and δ_L, such that $\beta_{PI} \geq \beta_L$ and $\delta_{PI} \geq \delta_L$, according to the condition

$$\delta_L = \frac{1}{\eta^3}\int_0^1 \left[\eta t - \sinh\eta t + (\cosh\eta t - 1)\tanh\eta\right]\left[f(U(t))\right]_{\beta=\beta_L} dt, \quad (53)$$

supplemented by the stationary condition obtained from the derivative of (53) with respect to δ and the maximum condition (52)

$$1 = \frac{1}{\eta^3}\int_0^1 \left[\eta t - \sinh\eta t + (\cosh\eta t - 1)\tanh\eta\right]\left[f'(U(t))\frac{\partial U(t)}{\partial\delta}\right]_{\beta=\beta_L} dt. \quad (54)$$

4.2. Upper bounds on the pull-in parameters

By using (46) and (51), Eq. (15) gives

$$\delta \geq \frac{1}{\eta^3}\int_0^1 \left[\eta t - \sinh\eta t + (\cosh\eta t - 1)\tanh\eta\right] f(L(t))dt, \quad (55)$$

being $f(u(t)) \geq f(L(t))$.

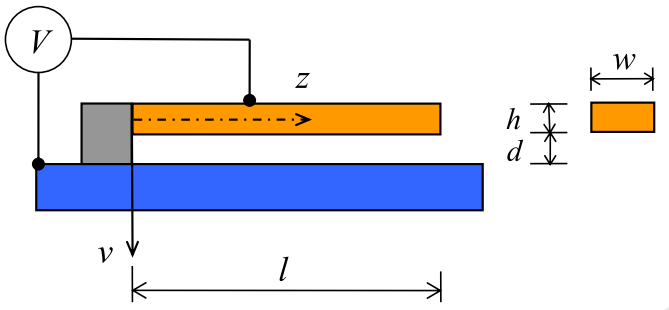

Fig. 1. A micro/nanocantilever under electrostatic actuation.

Table 1
Lower and upper analytical estimates of the pull-in parameters for a micro/nanocantilever with surface elasticity parameter $\eta = 0.5$, for different values of the parameters α_W, α_C, and γ.

$\eta = 0.5$		$\gamma = 0$				$\gamma = 1$				$\gamma = 2$			
α_W	α_C	δ_l	β_l	δ_u	β_u	δ_l	β_l	δ_u	β_u	δ_l	β_l	δ_u	β_u
0.0	0.0	0.4402	1.8254	0.4512	1.8591	0.4997	1.1025	0.5108	1.1211	0.5299	0.7979	0.5411	0.8108
0.0	0.2	0.3833	1.4028	0.3936	1.4357	0.4136	0.8188	0.4238	0.8366	0.4265	0.5806	0.4366	0.5928
0.0	0.4	0.3453	1.0252	0.3554	1.0579	0.3637	0.5866	0.3738	0.6044	0.3711	0.4118	0.3812	0.4241
0.0	0.6	0.3157	0.6752	0.3257	0.7078	0.3264	0.3807	0.3366	0.3986	0.3306	0.2655	0.3409	0.2778
0.0	0.8	0.2911	0.3448	0.3011	0.3773	0.2961	0.1922	0.3064	0.2101	0.2980	0.1333	0.3084	0.1457
0.0	1.0	0.2698	0.0295	0.2797	0.0620	0.2702	0.0163	0.2806	0.0342	0.2703	0.0112	0.2809	0.0236
0.0	0.0	0.4402	1.8254	0.4512	1.8591	0.4997	1.1025	0.5108	1.1211	0.5299	0.7979	0.5411	0.8108
0.2	0.0	0.4181	1.5297	0.4290	1.5636	0.4607	0.9103	0.4717	0.9290	0.4803	0.6522	0.4914	0.6652
0.4	0.0	0.3990	1.2416	0.4098	1.2755	0.4299	0.7302	0.4409	0.7490	0.4435	0.5195	0.4546	0.5325
0.6	0.0	0.3821	0.9597	0.3929	0.9937	0.4040	0.5589	0.4151	0.5778	0.4133	0.3953	0.4245	0.4085
0.8	0.0	0.3668	0.6831	0.3776	0.7172	0.3813	0.3943	0.3925	0.4134	0.3873	0.2776	0.3987	0.2910
1.0	0.0	0.3528	0.4110	0.3636	0.4453	0.3610	0.2354	0.3723	0.2547	0.3643	0.1651	0.3758	0.1786

Inequality (55) defines an upper bound on the relation between the electrostatic loading parameter β and the normalized pull-in deflection δ, both appearing in $L(t)$. The maxima of the electrostatic loading parameter β and of the corresponding tip deflection δ follow from stationarity of (55), as in (52). Accordingly, we get the upper bounds on the pull-in parameters, β_U and δ_U, such that $\beta_{PI} \leq \beta_U$and $\delta_{PI} \leq \delta_U$, where (Fig. 1).

$$\delta_U = \frac{1}{\eta^3}\int_0^1 [\eta t - \sinh\eta t + (\cosh\eta t - 1)\tanh\eta][f(L(t))]_{\beta=\beta_U} dt, \tag{56}$$

$$1 = \frac{1}{\eta^3}\int_0^1 [\eta t - \sinh\eta t + (\cosh\eta t - 1)\tanh\eta]\left[f'(L(t))\frac{\partial U(t)}{\partial \delta}\right]_{\beta=\beta_U} dt. \tag{57}$$

5. Results

Tables 1–3 present lower and upper bounds on the normalized pull-in voltage β_L and β_U and the corresponding values of the normalized pull-in deflection δ_L and δ_U for different values of the surface elastic energy coefficient η at fixed values for the normalized parameters γ, α_W, and α_C controlling the fringing effect and the intermolecular forces. As expected, for $\eta = 0$, namely neglecting the effect of the surface elastic energy, the analysis provides the results already presented in Radi et al. [28,29]. A purely numerical approach, based on the shooting method, has been used to obtain a reference solution to the boundary value problem (BVP) defined by the nonlinear ODE (1) and the boundary conditions (7).

The behaviour of the electrostatic loading parameter β against the nano-cantilever tip deflection $\delta = u(1)$ is reported in Fig. 2 for different values of the surface elastic energy coefficient η, in the absence of intermolecular forces, $\alpha_W = \alpha_C = 0$, and of fringing effects, $\gamma = 0$. The curves denote the numerical solution, whereas lower and upper analytical estimates of the pull-in parameters β_{PI} and δ_{PI} (i.e. of the maxima) are indicated by circles and dots, respectively. It can be observed that uncertainty, that is the distance between lower and upper analytical bounds, is very small in terms of both β and δ. Moreover, bounds well compare to the numerical solution. Interestingly, the pull-in voltage β_{PI} is an increasing function of η, thus denoting that the stiffening effect of surface elasticity leads to a higher pull-in voltage compared with that given by the classical theory of elasticity. Since the contribution of surface energy becomes more relevant as the size of the beam becomes smaller, its consideration is appreciable for microbeams and it definitely cannot be neglected when the beam size is reduced to the nanoscale. However, the effect of surface elasticity little affects the pull-in tip deflection δ_{PI}. Indeed, the latter stays almost constant at about 44% of the initial gap.

Table 2
Lower and upper analytical estimates of the pull-in parameters for a micro/nanocantilever with surface elasticity parameter $\eta = 1$, for different values of the parameters α_W, α_C, and γ.

$\eta = 1$		$\gamma = 0$				$\gamma = 1$				$\gamma = 2$			
α_W	α_C	δ_l	β_l	δ_u	β_u	δ_l	β_l	δ_u	β_u	δ_l	β_l	δ_u	β_u
0.0	0.0	0.4338	2.2723	0.4526	2.3426	0.4928	1.3731	0.5120	1.4121	0.5229	0.9939	0.5422	1.0212
0.0	0.2	0.3868	1.8443	0.4044	1.9131	0.4203	1.0826	0.4380	1.1202	0.4348	0.7698	0.4524	0.7958
0.0	0.4	0.3538	1.4562	0.3710	1.5244	0.3760	0.8395	0.3933	0.8769	0.3851	0.5915	0.4024	0.6173
0.0	0.6	0.3275	1.0939	0.3445	1.1617	0.3423	0.6222	0.3596	0.6595	0.3483	0.4356	0.3656	0.4613
0.0	0.8	0.3055	0.7504	0.3223	0.8180	0.3148	0.4222	0.3320	0.4595	0.3184	0.2941	0.3358	0.3198
0.0	1.0	0.2862	0.4217	0.3029	0.4891	0.2911	0.2351	0.3083	0.2723	0.2930	0.1631	0.3104	0.1888
0.0	0.0	0.4338	2.2723	0.4526	2.3426	0.4928	1.3731	0.5120	1.4121	0.5229	0.9939	0.5422	1.0212
0.2	0.0	0.4160	1.9758	0.4346	2.0462	0.4611	1.1795	0.4800	1.2186	0.4822	0.8467	0.5013	0.8740
0.4	0.0	0.4003	1.6856	0.4187	1.7561	0.4352	0.9961	0.4540	1.0354	0.4508	0.7107	0.4698	0.7380
0.6	0.0	0.3861	1.4007	0.4044	1.4713	0.4129	0.8206	0.4318	0.8601	0.4245	0.5825	0.4436	0.6101
0.8	0.0	0.3731	1.1204	0.3914	1.1912	0.3932	0.6514	0.4121	0.6911	0.4017	0.4605	0.4208	0.4882
1.0	0.0	0.3611	0.8442	0.3793	0.9151	0.3754	0.4875	0.3944	0.5274	0.3813	0.3433	0.4006	0.3712

Table 3
Lower and upper analytical estimates of the pull-in parameters for a micro/nanocantilever with surface elasticity parameter $\eta = 1.5$, for various values of the parameters α_W, α_C, and γ.

$\eta = 1.5$		$\gamma = 0$				$\gamma = 1$				$\gamma = 2$			
α_W	α_C	δ_l	β_l	δ_u	β_u	δ_l	β_l	δ_u	β_u	δ_l	β_l	δ_u	β_u
0.0	0.0	0.4249	2.9797	0.4575	3.1436	0.4832	1.8017	0.5167	1.8929	0.5130	1.3046	0.5468	1.3684
0.0	0.2	0.3882	2.5462	0.4192	2.7072	0.4254	1.5039	0.4565	1.5924	0.4417	1.0731	0.4728	1.1342
0.0	0.4	0.3608	2.1463	0.3911	2.3058	0.3875	1.2481	0.4179	1.3356	0.3987	0.8832	0.4291	0.9436
0.0	0.6	0.3385	1.7697	0.3683	1.9283	0.3582	1.0168	0.3883	1.1040	0.3662	0.7152	0.3964	0.7754
0.0	0.8	0.3195	1.4107	0.3489	1.5686	0.3339	0.8026	0.3639	0.8895	0.3396	0.5618	0.3698	0.6219
0.0	1.0	0.3028	1.0657	0.3320	1.2231	0.3129	0.6012	0.3429	0.6880	0.3169	0.4193	0.3471	0.4792
0.0	0.0	0.4249	2.9797	0.4575	3.1436	0.4832	1.8017	0.5167	1.8929	0.5130	1.3046	0.5468	1.3684
0.2	0.0	0.4114	2.6824	0.4438	2.8464	0.4589	1.6067	0.4920	1.6980	0.4815	1.1558	0.5149	1.2195
0.4	0.0	0.3991	2.3900	0.4313	2.5541	0.4382	1.4200	0.4711	1.5115	0.4560	1.0162	0.4892	1.0800
0.6	0.0	0.3879	2.1019	0.4199	2.2663	0.4200	1.2399	0.4529	1.3317	0.4342	0.8835	0.4674	0.9476
0.8	0.0	0.3774	1.8177	0.4093	1.9822	0.4036	1.0653	0.4365	1.1575	0.4149	0.7563	0.4482	0.8206
1.0	0.0	0.3676	1.5370	0.3994	1.7017	0.3887	0.8955	0.4216	0.9881	0.3976	0.6337	0.4310	0.6983

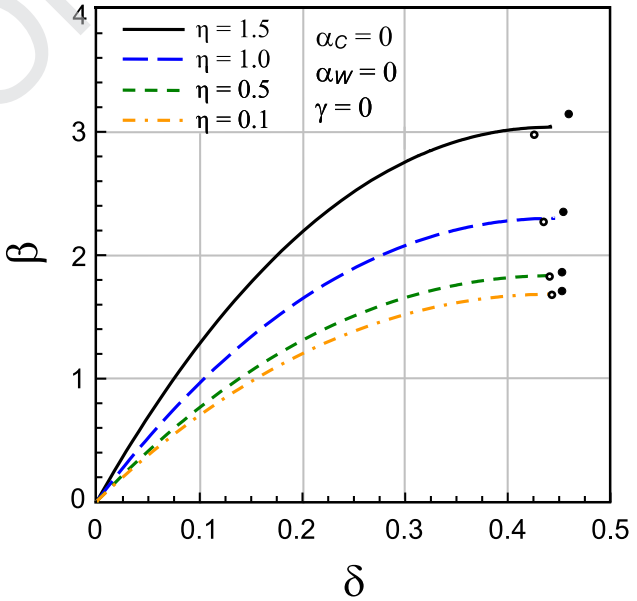

Fig. 2. Plot of the electrostatic loading parameter β against the tip deflection δ obtained by numerical integration of the BVP, for various values of the surface elasticity parameter η, for negligible intermolecular forces $\alpha_W = \alpha_C = 0$ and negligible fringing effect $\gamma = 0$. Lower and upper analytical estimates of the pull-in parameters are indicated by small circles and small points, respectively.

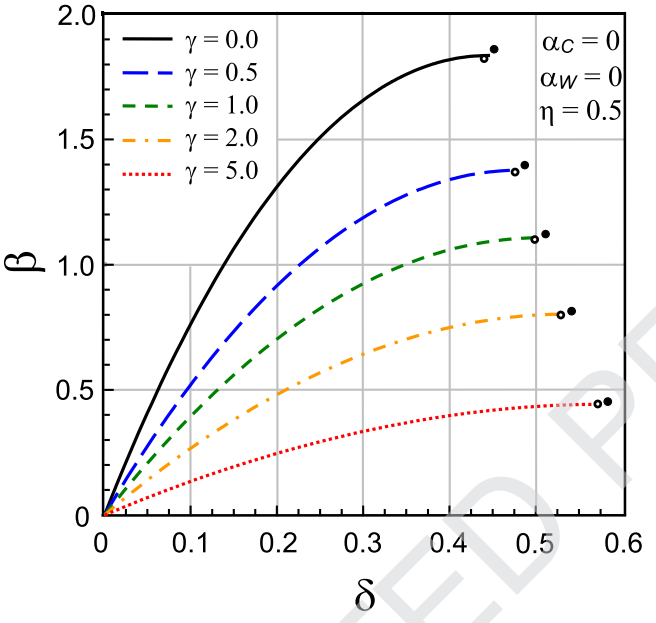

Fig. 3. Plot of the cantilever tip deflection δ against the electrostatic loading parameters β obtained by numerical integration of the BVP, for $\eta = 0.5$ and for different values of the fringing effect γ. Lower and upper analytical estimates of the pull-in parameters are indicated by small circles and small points, respectively.

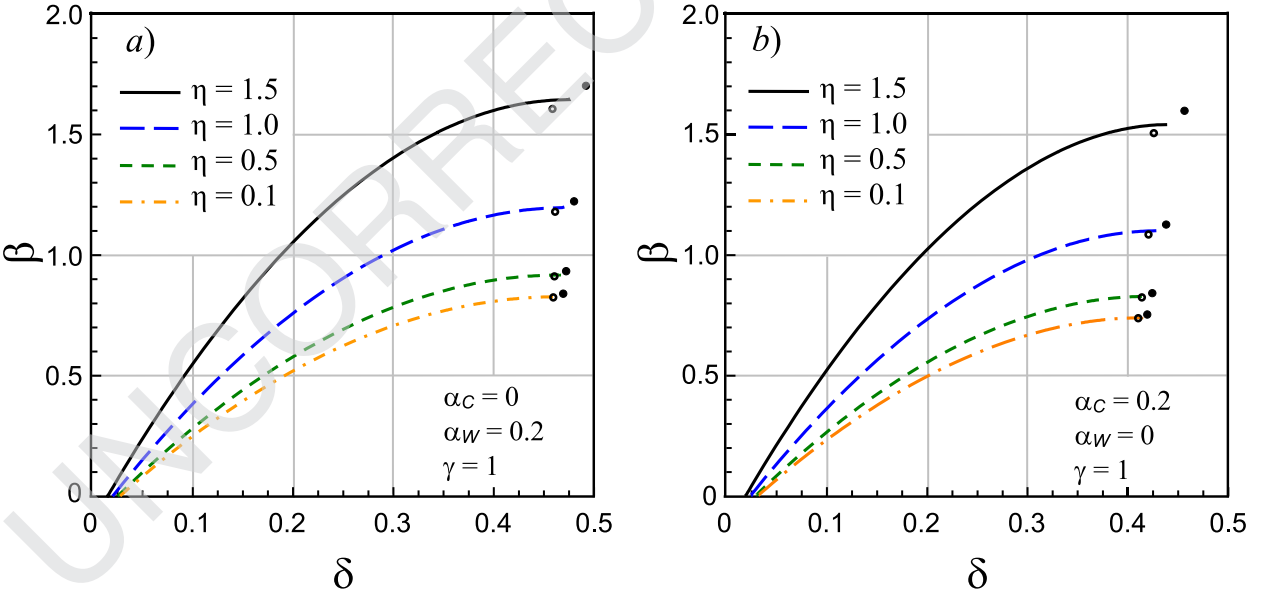

Fig. 4. Plot of the electrostatic loading parameter β against the cantilever tip deflection δ obtained by numerical integration of the BVP, for different values of the surface elasticity parameter η, for the fringing effect $\gamma = 1$ and for vdW parameters $\alpha_W = 0.2$ (a) or for Casimir parameters $\alpha_C = 0.2$ (b). Lower and upper analytical estimates of the pull-in parameters are indicated by small circles and small points, respectively.

Fig. 3 shows the effects of the fringing coefficient γ on the pull-in parameters at $\eta = 0.5$ for the surface energy contribution and no vdW or Casimir force. As expected, the largest pull-in voltage is attained for small fringing, that occurs when the separation gap between the electrodes, *d*, is much smaller than the beam width, *w*. As the effect of the fringing field becomes more pronounced, the pull-in voltage β_{PI} decreases, whereas, interestingly, the corresponding pull-in deflection δ_{PI} increases.

Fig. 4 couples the surface elasticity parameter η and the fringing field $\gamma = 1$ with either vdW or Casimir forces, α_W or α_C. A significant reduction of the pull-in voltage is observed with respect to the results of Fig. 2, due to combined effects considered here. In particular, intermolecular forces significantly increase the beam deflection and consequently pull-in in-

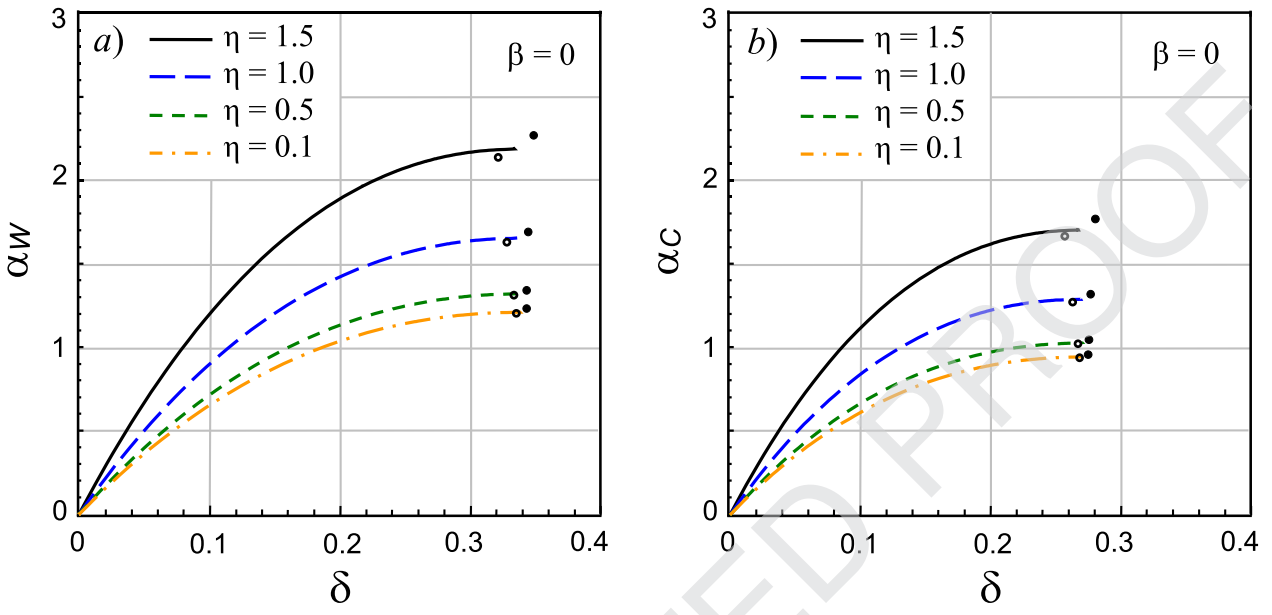

Fig. 5. Plot of the vdW and of the Casimir parameters α_W and α_C, respectively, against the cantilever tip deflection δ obtained by numerical integration of the BVP, for vanishing electrostatic loading parameter ($\beta = 0$) and for various values of the surface elasticity parameter η. Lower and upper analytical estimates of the pull-in parameters are denoted by small circles and small points, respectively.

Table 4
Lower and upper analytical estimates of α_W, α_C, and δ for different values of the surface elasticity parameter η, for a freestanding micro/nanocantilever ($\beta = 0$).

η	α_{Wl}	δ_{Wl}	α_{Wu}	δ_{Wu}	α_{Cl}	δ_{Cl}	α_{Cu}	δ_{Cu}
0.0	1.1967	0.3350	1.2171	0.3423	0.9326	0.2694	0.9492	0.2756
0.1	1.2025	0.3350	1.2218	0.3423	0.9372	0.2693	0.9528	0.2756
0.5	1.3078	0.3332	1.3339	0.3425	1.0191	0.2679	1.0403	0.2758
1.0	1.6273	0.3282	1.6813	0.3438	1.2679	0.2637	1.3116	0.2769
1.2	1.8087	0.3255	1.8842	0.3450	1.4091	0.2615	1.4700	0.2780
1.5	2.1327	0.3211	2.2584	0.3482	1.6611	0.2579	1.7626	0.2807

stability occurs at lower applied voltage. If the contributions of fringing and intermolecular forces are neglected, the pull-in voltage may be considerably over-estimated, so that unexpected damage may occur during device operations. Remarkably, Fig. 4 shows that intermolecular surface forces produce an initial deflection of the nano-beam in the absence of applied electric voltage, namely for $\beta = 0$, even accounting for surface energy. This behaviour is explored in Fig. 5 that plots the tip deflection δ against the vdW and Casimir parameters, α_W and α_C, at different values of the surface elasticity parameter η, in the absence of electrostatic actuation, $\beta = 0$. Plots reveal that pull-in instability kicks in upon reaching the critical threshold α_{WPI} and α_{CPI} even when no electric voltage is applied to the electrodes. Interestingly, although threshold values considerably increase with the introduction of surface elasticity effect through the parameter η, the latter has no appreciable influence on the normalized pull-in tip deflection δ_{PI}, meaning that instability occurs upon reaching a critical value of the ratio between tip deflection and initial gap. This suggests that initial gap appears to be the most important design parameter in the system. Comparing Fig. 5(a) and (b), it can be noted that vdW effects trigger pull-in instability at greater tip deflection (and therefore at smaller separation gap between the electrodes) than it does Casimir attraction. The critical normalized maximum deflection δ_{PI} caused by the sole effect of the vdW force is indeed about 3.4 and that caused by the sole effect of the Casimir force is about 2.7. These results correspond to critical gaps of about 66% and 73% of the initial gap d in the absence of every kind of forces, respectively. This outcome confirms the well-known result that vdW forces are effective at shorter range than Casimir's, and thus the former are significant at the microscale whereas the latter are effective at the nanoscale only. Also, for the freestanding case, the analytical estimates of α_{WPI} and α_{CPI}, and the corresponding pull-in deflection δ_{PI} agree very well with the numerical results.

Lower and upper estimates of critical vdW and Casimir parameters α_{WPI} and α_{CPI} and tip deflection δ_{PI} for a freestanding nanocantilever can be found in Table 4 for different values of η. These results confirm that pull-in instability is hindered as the surface elasticity parameter η increases, as already observed from Fig. 2. As already observed in Fig. 5, the normalized pull-in tip deflection δ_{PI} is higher for vdW than for Casimir forces, whereas it is almost independent of η.

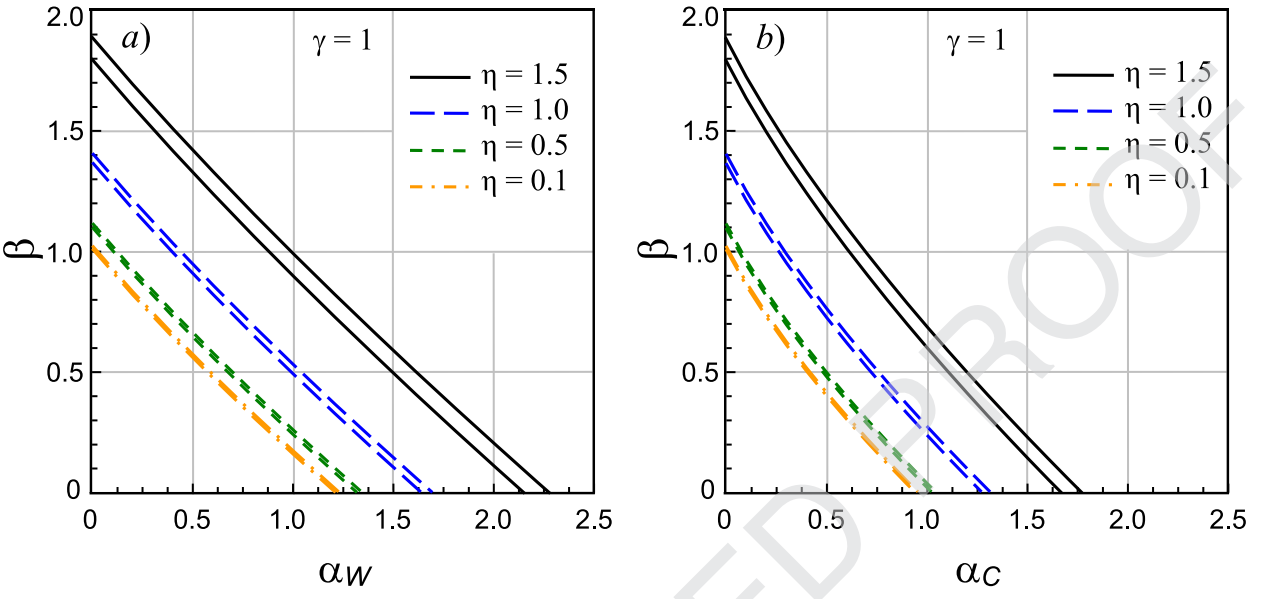

Fig. 6. Influence of the van der Waals (*a*) and Casimir (*b*) forces on the pull-in voltage parameter β, for different values of the surface elasticity parameter η.

The behaviour of the upper and lower approximation to the pull-in voltage, respectively β_U and β_L, as a function of α_W and α_C, is investigated in Fig. 6 for different values of the surface elasticity parameter η. There, it can be observed that both the pull-in parameter and the threshold value of the intermolecular coefficients increase when η increases, accounting for the fact that surface energy opposes pull-in instability regardless of whether it comes from electrostatic potential or from intermolecular action. In contrast, increasing the parameter α_W and α_C, the pull-in voltage is significantly reduced until the intermolecular parameters attain their threshold values α_{WPI} and α_{CPI} attained at zero applied voltage. In fact, when intermolecular surface attractions overcome the elastic restoring force of the nano-beam, negative values of β, namely repulsive electrostatic forces, are required to prevent pull-in instability. Again, lower and upper estimates are very close and accurate, especially when η ranges below 2 and regardless of intermolecular forces.

The effect of the surface energy parameter η on the lower and upper bound of the pull-in voltage β_{PI} and of the tip deflection δ_{PI} is presented, for vanishing fringing and intermolecular forces (that is for $\gamma = \alpha_W = \alpha_C, = 0$), in Fig. 7a and 7b, respectively. Fig. 7a shows that the lower and upper analytical bounds on the pull-in parameter β are very close to each other and monotonically increase along with the surface energy η. Conversely, the lower and upper bound on the normalized pull-in tip deflection weakly decreases as the surface elasticity contribution strengthens, see Fig. 7b, while remaining at about 44% of the initial gap. Here, the analytical lower and upper bounds are still close but they reveal an opposite trend, whereby the lower bound decreases and the upper bound increases. As a consequence, accurate pull-in bounds are available for tip deflection only inasmuch as sufficiently small values of η are considered.

5.1. Approximated analytical relations for the pull-in parameters

On the basis of the developed analytical bounds, approximate relations are here proposed for easy and simple design of the pull-in characteristics of an electrostatically actuated nano-cantilever taking into account the surface elasticity effect proportional to parameter η.

When the effects of the fringing field and of intermolecular surface forces are neglected, the following approximate relations

$$\beta = 1.69 + 0.61\,\eta^2, \qquad \delta = \begin{cases} 0.4426 - 0.01057\,\eta^2 + 0.0018\,\eta^3 & \text{for} \quad \eta \le 2, \\ 0.4523 - 0.0189\,\eta & \text{for} \quad \eta > 2. \end{cases} \tag{58}$$

describe the evolution of the pull-in characteristics β and δ in terms of the surface elasticity parameter η. The accuracy of these relations is presented in Fig. 8a and 8b, respectively for voltage and tip deflection, where circles and dots indicate lower and upper analytical bounds. The first of the approximants (58) is determined by least-square polynomial interpolation of the analytical bounds in the range for η from 0 to 2. In contrast, the approximant for the tip deflection is obtained by interpolation of the lower bound only, since lower and upper bounds display opposite trends and no unique accurate interpolant exists.

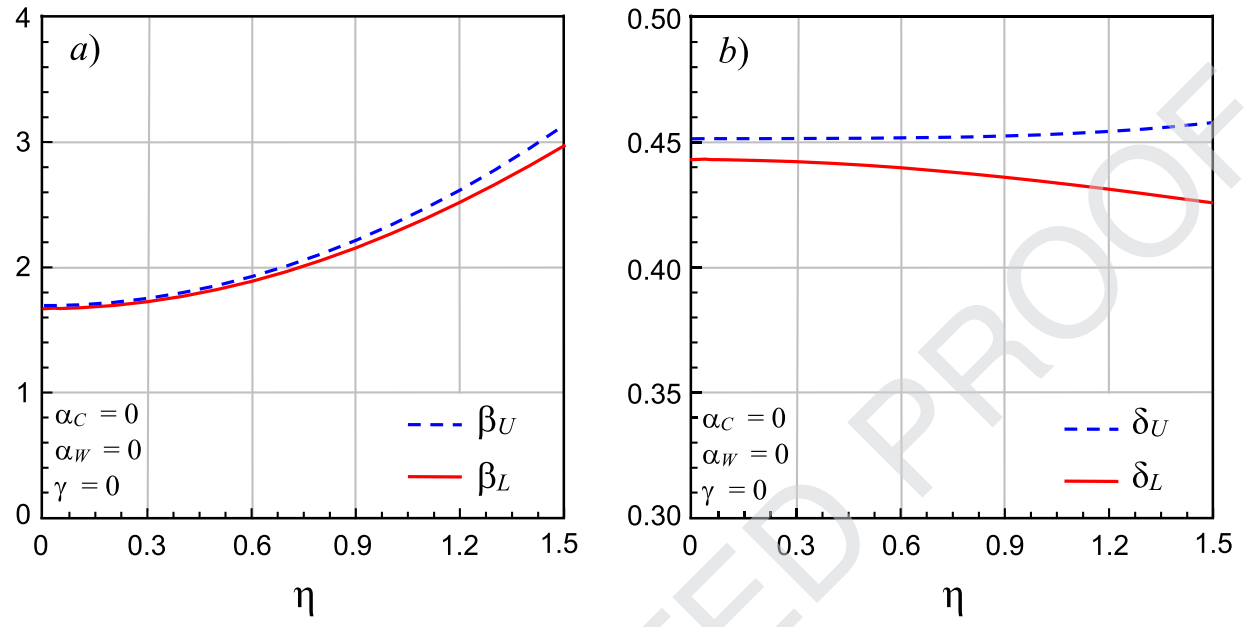

Fig. 7. Plot of the lower β_L and upper β_U bound for the pull-in voltage (a) and of the relevant cantilever tip deflection δ_L and δ_U (b) with respect to the surface elasticity parameter η for a micro-nanocantilever where the effects of fringing and intermolecular surface forces are absent.

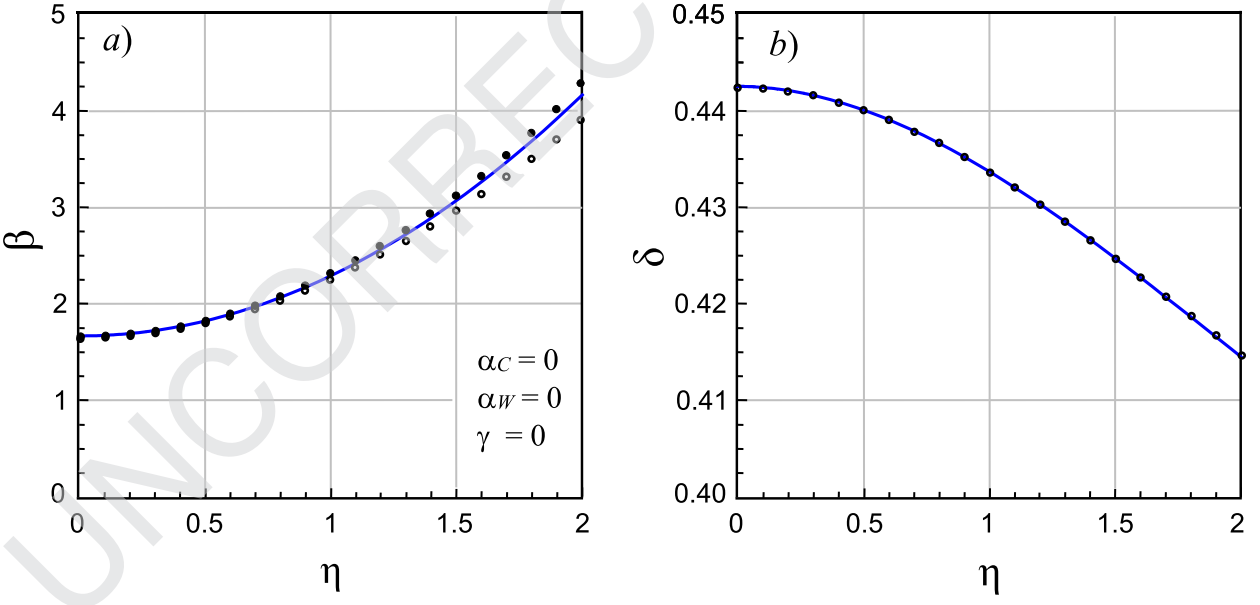

Fig. 8. Plot of the pull-in voltage β and cantilever tip deflection δ against the surface elasticity parameter η, where the effects of fringing and intermolecular surface forces are neglected. Lower and upper analytical estimates of the pull-in parameters are denoted by small circles and small points, respectively. Blue lines show the pull-in values provided by the approximated relations (58).

For a freestanding nano-cantilever, namely in the absence of applied electrostatic voltage, $\beta = 0$, the following quadratic relations provide a very good approximation for the threshold vdW and Casimir parameters

$$\alpha_{WPI} = 1.21 + 0.43\,\eta^2, \quad \alpha_{CPI} = 0.94 + 0.34\,\eta^2. \tag{59}$$

As it appears from Fig. 9, expressions (59) fit lower and upper analytical bounds very well, in the considered range of the parameter η.

More involved relations are demanded for approximating the relationships between the pull-in voltage β and the surface elasticity parameter η in the presence of intermolecular attraction (but in the absence of the fringing field), namely for non-

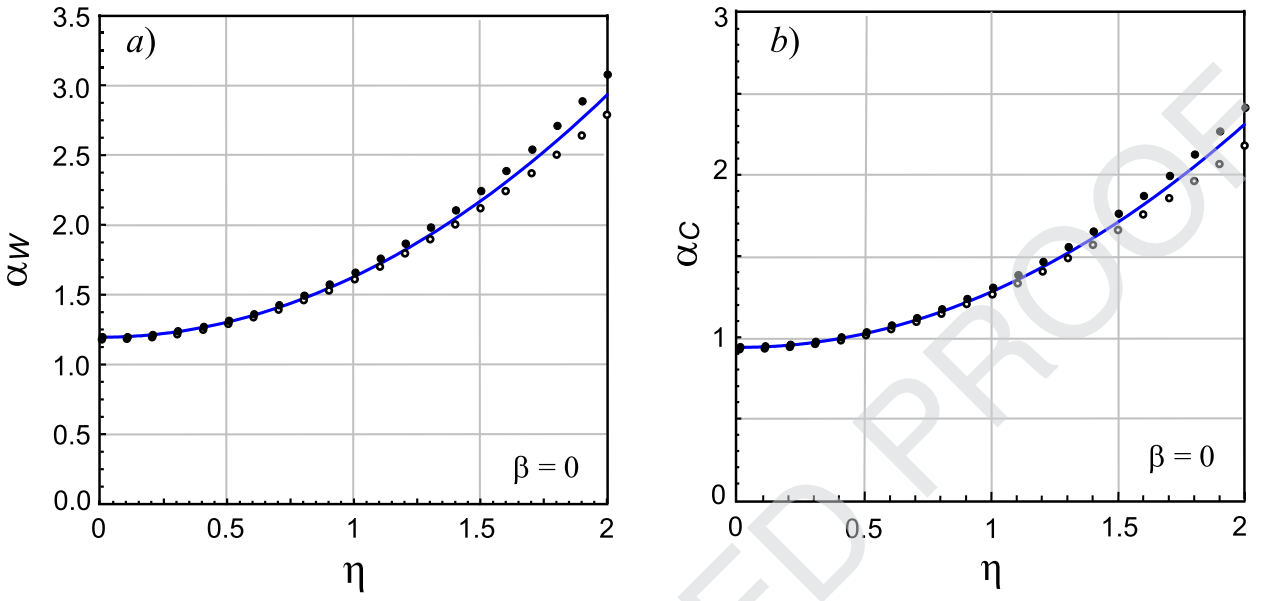

Fig. 9. Relationships between vdW and Casimir parameters α_W and α_C and the surface elasticity parameter η, for vanishing electrostatic loading parameter ($\beta = 0$). Lower and upper analytical estimates of the pull-in parameters are denoted by small circles and small points, respectively. Blue lines show the pull-in values for intermolecular forces provided by approximated Eq. (59).

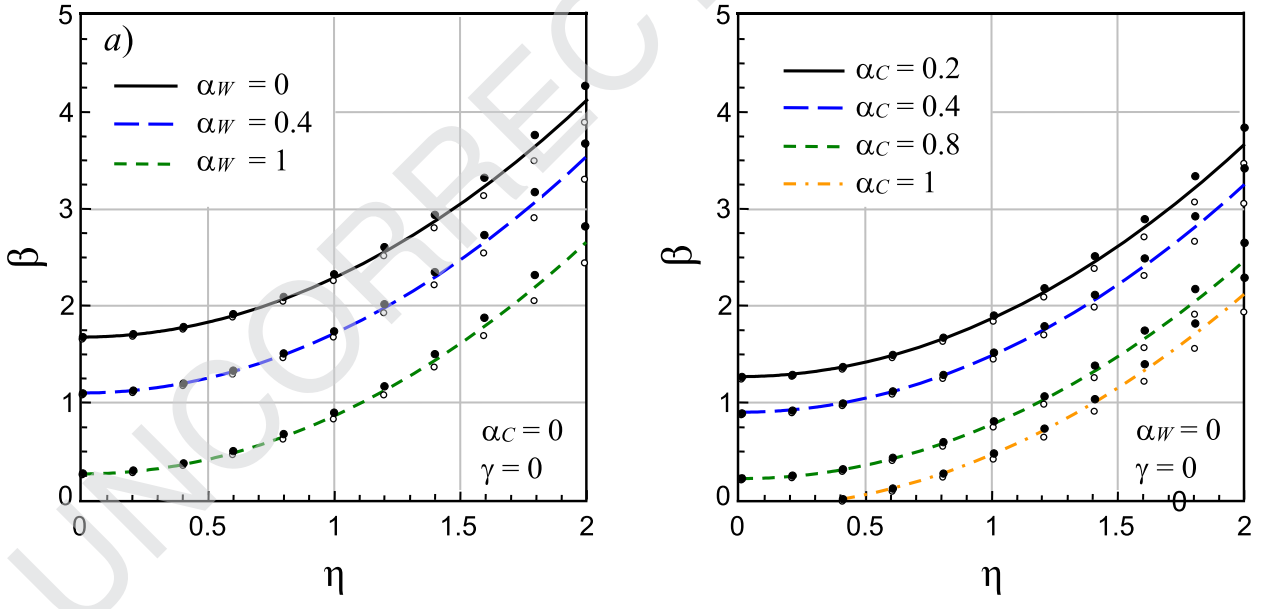

Fig. 10. Relationships between parameters β and the surface elasticity parameter η, for various values of the vdW and Casimir parameters α_W and α_C, for negligible fringing effect $\gamma = 0$. Lower and upper analytical estimates of the pull-in parameters are denoted by small circles and small points, respectively. Solid and dashed curves show the pull-in values provided by approximated Eqs. (60) and (61).

zero values of the vdW parameter α_W and of the Casimir parameter α_C:

$$\beta = 1.6935 - 1.4858\alpha_W + 0.0745\alpha_W^2 + (0.6043 - 0.017\alpha_W^2 + 0.0052\alpha_W^3)\,\eta^2, \tag{60}$$

$$\beta = 1.6885 - 2.1066\alpha_C + 0.3291\alpha_C^2 + (0.6033 - 0.1021\alpha_C^2 + 0.051\alpha_C^3)\,\eta^2. \tag{61}$$

In both formulae, a relation that is quadratic in the parameter η is adopted, yet coefficients of the approximating polynomial explicitly depend on the intermolecular surface parameters α_W or α_C. This fitting is dealt with in a double stage process. First, families of lower and upper analytical bounds are obtained as a function of the elastic surface energy parameter η in the range [0, 2], at 0.2 steps, for different sets of intermolecular action parameters α_W and α_C. Each data set in

a family is fitted by a quadratic polynomial. Second, the NonlinearModelFit function of *Mathematica®* is employed to determine the best functional dependence of the polynomial coefficients to accommodate for the family of approximants. The corresponding curves, plotted in Fig. 10a and 10b, exhibits excellent agreement with the analytical lower and upper estimates, indicated in the picture with circles and dots, respectively. As already observed, for high values of the intermolecular surface forces, pull-in instability occurs in the absence of electrostatic field, $\beta = 0$, provided that the stabilizing effect of the surface elasticity parameter η is small enough. The approximate relations (60) and (61) constitute powerful and easy-to-use tools for safe design of nano-switches.

6. Conclusions

We present sharp lower and upper analytical bounds on the deflection of an electrically-actuated micro/nano-cantilever, taking into account the effect of surface elastic energy, which is especially relevant at small length-scales. The bounding solutions to this non-linear problem are obtained by carefully estimating the cantilever deflection and its derivatives. In this approach, consideration of surface elasticity provides considerable complication, given that this contribution operates against the electrostatic action and prevents a simple convex shape for the deflection. Correspondingly, simple estimates for the second derivative of the deflection are not available. Analytical bounds compare very favourably with the results of direct numerical integration of the nonlinear BVP. In particular, they well capture the pull-in voltage and the pull-in gap, and show that only the former is strongly increased by surface elastic energy. However, the accuracy of the estimates deteriorates as the role of surface elasticity becomes more pronounced. This outcome is a result of the complex behaviour of the deflection shape, which affects in the negative any solution method.

Simple approximate relations are proposed as ready-to-use design formulae for framing the pull-in parameters of newly conceived devices. In particular, they provide the limiting electrode gap and the maximum operative cantilever length which are possible for a given material parameter set. These bounds are crucial to avoid unwarranted operation of MEMS and NEMS actuators within the given driving voltage range, which may occur if devices are designed based on the classical theory of elasticity.

It is further believed that this study may fill in the gap between purely numerical solutions of the governing equation, that shed no light on the role of the parameters, and crude one-degree-of-freedom approximations, which lack the accuracy required to adequately describe the behaviour of the system until pull-in instability occurs. This is especially true when surface elastic energy is considered, for then deflection is generally complicated and far from any classical deflection mode of a cantilever beam.

Acknowledgment

Support from the Italian "Gruppo Nazionale di Fisica Matematica" INdAM-GNFM is gratefully acknowledged.

Appendix A

Lemma A. Let the function $h(x)$ be continuous up to the third derivative for $x \in [0, 1]$ and satisfy the following conditions

$$h(0) = 0, \quad h(1) = 0, \quad h'(0) = 0, \quad h''(1) = 0, \quad h'''(1) = 0, \tag{A.1}$$

and

$$h^{V}(x) \leq 0, \quad \text{for } x \in [0, 1] \tag{A.2}$$

then

$$h(x) \geq 0, \quad \text{for } x \in [0, 1] \tag{A.3}$$

Lemma B. Let the function $g(x)$ be continuous up to the third derivative for $x \in [0, 1]$ and satisfy the following conditions

$$g(0) = 0, \quad g(1) = 0, \quad g'(0) = 0, \quad g''(1) = 0. \tag{A.4}$$

and

$$g^{IV}(x) \geq 0, \quad \text{for } x \in [0, 1] \tag{A.5}$$

then

$$g(x) \geq 0, \quad \text{for } x \in [0, 1] \tag{A.6}$$

Proof. The proofs are given in Radi et al. [28,29].

Appendix B

Expressions for the functions introduced in (34)

$$a(x) = \frac{6x^5 - x^6}{720\,\eta^2} + \frac{(1+\eta\sinh\eta)(\cosh\eta x - \eta^4x^4/24)}{\eta^8\cosh\eta} - \frac{\sinh\eta x}{\eta^7} = b(x) - \frac{(1+\eta\sinh\eta)\,x^4}{24\eta^4\cosh\eta}, \tag{B.1}$$

$$b(x) = \frac{6x^5 - x^6}{720\,\eta^2} + \frac{1+\eta\sinh\eta}{\eta^8\cosh\eta}\cosh\eta x - \frac{\sinh\eta x}{\eta^7}, \tag{B.2}$$

$$c(x) = \frac{15\,\cosh\eta(1-2x) + 4800\,\cosh\eta(1-x) + 960\,\eta x\,\sinh\eta(1-x) + 4\eta^5x^5\sinh\eta}{960\,\eta^6\cosh\eta}, \tag{B.3}$$

$$\begin{aligned} d(x) &= \frac{15\,\cosh\eta(1-2x) + 4800\,\cosh\eta(1-x) - 960\,\eta(1-x)\,\sinh\eta(1-x) + 4\eta^5x^5\sinh\eta - 960\,\cosh\eta x}{960\,\eta^6\cosh\eta} \\ &= c(x) - \frac{\cosh\eta x + \eta\sinh\eta(1-x)}{\eta^6\cosh\eta}. \end{aligned} \tag{B.4}$$

References

[1] O.Y. Loh, H.D. Espinosa, Nanoelectromechanical contact switches, Nat. Nanotechnol. 7 (2012) 283–295.
[2] Y.T. Beni, A. Koochi, M. Abadyan, Theoretical study of the effect of Casimir force, elastic boundary conditions and size dependency on the pull-in instability of beam-type NEMS, Phys. E: Lowdim. Sys. Nanostruct. 43 (2011) 979–988.
[3] G.-F. Wang, X.-Q. Feng, Surface effects on buckling of nanowires under uniaxial compression, Appl. Phys. Lett. 94 (2009) 141913.
[4] H. Sadeghian, C.K. Yang, J.F.L. Goosen, E. van der Drift, A. Bossche, P.J. French, F. van Keulen, Characterizing size-dependent effective elastic modulus of silicon nanocantilevers using electrostatic pull-in instability, Appl. Phys. Lett. 94 (2009) 221903.
[5] M. Baghani, Analytical study on size-dependent static pull-in voltage of microcantilevers using the modified couple stress theory, Int. J. Eng. Sci. 54 (2012) 99–105.
[6] N. Challamel, I. Elishakoff, Surface stress effects may induce softening: Euler-Bernoulli and Timoshenko buckling solutions, Phys. E: Low-Dimens. Syst. Nanostruct. 44 (2012) 1862–1867.
[7] S. Cuenot, C. Frétigny, S. Demoustier-Champagne, B. Nysten, Surface tension effect on the mechanical properties of nanomaterials measured by atomic force microscopy, Phys. Rev. B 69 (2004) 165410.
[8] J.-S. Duan, R. Rach, A pull-in parameter analysis for the cantilever NEMS actuator model including surface energy, fringing field and Casimir effects, Int. J. Solids Struct. 50 (2013) 3511–3518.
[9] J. He, C.M. Lilley, Surface effect on the elastic behavior of static bending nanowires, Nano Lett. 8 (2008) 1798–1802.
[10] J.B. Ma, L. Jiang, S.F. Asokanthan, Influence of surface effects on the pull-in instability of NEMS electrostatic switches, Nanotechnology 21 (2010) 505708.
[11] A.W. McFarland, M.A. Poggi, M.J. Doyle, L.A. Bottomley, J.S. Colton, Influence of surface stress on the resonance behavior of microcantilevers, Appl. Phys. Lett. 87 (2005) 053505.
[12] H.S. Park, Surface stress effects on the critical buckling strains of silicon nanowires, Comput. Mater. Sci. 51 (2012) 396–401.
[13] M.A. Eltaher, M.E. Khater, S.A Emam, A review on nonlocal elastic models for bending, buckling, vibrations, and wave propagation of nanoscale beams, Appl. Math. Model. 40 (2016) 4109–4128.
[14] S.A. Emam, A general nonlocal nonlinear model for buckling of nanobeams, Appl. Math. Model. 37 (2013) 6929–6939.
[15] A.C. Eringen, Nonlocal Continuum Field Theories, Springer-Verlag, New York, 2002.
[16] G. Mikhasev, A. Nobili , On the solution of the purely nonlocal theory of beam elasticity as a limiting case of the two-phase theory, Int. J. Solids Struct. (2020) In press.
[17] M.E. Gurtin, A.I. Murdoch, A continuum theory of elastic material surfaces, Arch. Ration. Mech. Anal. 57 (1975) 291–323.
[18] M.E. Gurtin, A.I. Murdoch, Surface stress in solids, Int. J. Solids Struct. 14 (1978) 431–440.
[19] W.C. Chuang, H.L. Lee, P.Z. Chang, Y.C. Hu, Review on the modeling of electrostatic MEMS, Sensors 10 (2010) 6149–6171.
[20] Y. Zhang, Y.P. Zhao, Numerical and analytical study on the pull-in instability of micro-structure under electrostatic loading, Sens. Actuat. A: Phys. 127 (2006) 366–380.
[21] A. Ramezani, A. Alasty, J. Akbari, Influence of van der Waals force on the pull-in parameters of cantilever type nanoscale electrostatic actuators, J. Microsyst. Technol. 12 (2006) 1153–1161.
[22] A. Ramezani, A. Alasty, J. Akbari, Closed-form solutions of the pull-in instability in nanocantilevers under electrostatic and intermolecular surface forces, Int. J. Solids Struct. 44 (2007) 4925–4941.
[23] J. Duan, Z. Li, J. Liu, Pull-in instability analyses for NEMS actuators with quartic shape approximation, Appl. Math. Mech. 37 (2016) 303–314.
[24] J.-S. Duan, R. Rach, A.-M. Wazwaz, Solution of the model of beam-type micro-and nano-scale electrostatic actuators by a new modified Adomian decomposition method for nonlinear boundary value problems, Int. J. Non-Lin. Mech. 49 (2013) 159–169.
[25] Y. Fu, J. Zhang, Size-dependent pull-in phenomena in electrically actuated nanobeams incorporating surface energies, Appl. Math. Model. 35 (2011) 941–951.
[26] K.F. Wang, B.L. Wang, Influence of surface energy on the non-linear pull-in instability of nano-switches, Int. J. Non-Lin. Mech. 59 (2014) 69–75.
[27] K.F. Wang, B.L. Wang, A general model for nano-cantilever switches with consideration of surface effects and nonlinear curvature, Phys. E: Low-Dimens. Syst. Nanostruct. 66 (2015) 197–208.
[28] E. Radi, G. Bianchi, L. di Ruvo, Upper and lower bounds for the pull-in parameters of a micro- or nanocantilever on a flexible support, Int. J. Nonlin. Mech. 92 (2017) 176–186.
[29] E. Radi, G. Bianchi, L. di Ruvo, Analytical bounds for the electromechanical buckling of a compressed nanocantilever, Appl. Math. Model. 59 (2018) 571–572.
[30] G. Bianchi, E. Radi, Analytical estimates of the pull-in voltage for carbon nanotubes considering tip-charge concentration and intermolecular forces, Meccanica 55 (2020) 193–209.
[31] A. Farrokhabadi, A. Mohebshahedin, R. Rach, J.S. Duan, An improved model for the cantilever NEMS actuator including the surface energy, fringing field and Casimir effects, Phys. E: Low-Dimens. Syst. Nanostruct. 75 (2016) 202–209.
[32] A. Koochi, A. Kazemi, F. Khandani, M. Abadyan, Influence of surface effects on size-dependent instability of nano-actuators in the presence of quantum vacuum fluctuations, Phys. Scr. 85 (2012) 035804.